

Semiautomated Production of Cell-Free Biosensors

Dylan M. Brown,[#] Daniel A. Phillips,[#] David C. Garcia, Anibal Arce, Tyler Lucci, John P. Davies, Jr., Jacob T. Mangini, Katherine A. Rhea, Casey B. Bernhards, John R. Biondo, Steven M. Blum, Stephanie D. Cole, Jennifer A. Lee, Marilyn S. Lee, Nathan D. McDonald, Brenda Wang, Dale L. Perdue, Xavier S. Bower, Walter Thavarajah, Ashty S. Karim, Matthew W. Lux, Michael C. Jewett, Aleksandr E. Miklos,^{*} and Julius B. Lucks^{*}

Cite This: *ACS Synth. Biol.* 2025, 14, 979–986

Read Online

ACCESS |



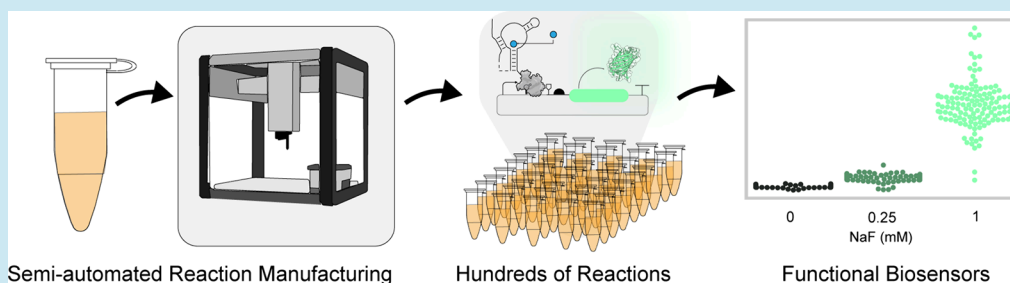
Metrics & More



Article Recommendations



Supporting Information



ABSTRACT: Cell-free synthetic biology biosensors have potential as effective *in vitro* diagnostic technologies for the detection of chemical compounds, such as toxins and human health biomarkers. They have several advantages over conventional laboratory-based diagnostic approaches, including the ability to be assembled, freeze-dried, distributed, and then used at the point of need. This makes them an attractive platform for cheap and rapid chemical detection across the globe. Though promising, a major challenge is scaling up biosensor manufacturing to meet the needs of their multiple uses. Currently, cell-free biosensor assembly during lab-scale development is mostly performed manually by the operator, leading to quality control and performance variability issues. Here we explore the use of liquid-handling robotics to manufacture cell-free biosensor reactions. We compare both manual and semiautomated reaction assembly approaches using the Opentrons OT-2 liquid handling platform on two different cell-free gene expression assay systems that constitutively produce colorimetric (LacZ) or fluorescent (GFP) signals. We test the designed protocol by constructing an entire 384-well plate of fluoride-sensing cell-free biosensors and demonstrate that they perform close to expected detection outcomes.

KEYWORDS: Cell-free biosensors, cell-free systems, point-of-use manufacturing, fluoride riboswitch, automation

INTRODUCTION

Environmental chemical hazards are a major global threat to human and environmental health—affecting air, water, soil, and food quality globally.^{1–5} Exposure to environmental hazards leads to poor human health outcomes, such as asthma, mental illness, birth defects, cancer, chronic illness, cardiovascular disease, or death.^{6–10} Current technologies for assessing environmental hazards often require laboratory facilities, electronic devices, and technical expertise. Though a variety of government organizations monitor contaminants, their methods of detection often include analytical techniques such as gas chromatography, liquid chromatography, and mass spectrometry.^{11,12} Field-deployable technologies are prone to similar user difficulties, requiring expertise in the field or complex data analysis, with modern methods still using electrical signals, chromatography, or spectroscopic devices.^{13–16} These types of detection methods are often inaccessible to under-resourced locations and difficult to use

for individuals without technical expertise who would benefit most from easy-to-use detection methods. Additionally, these detection methods lack scalability in that detection reliant on analytical devices is often not rapid and cannot be mass-produced and distributed to individuals easily and cheaply.

Cell-free gene expression systems can be used as a powerful strategy to cheaply create ready-to-use diagnostic devices that are able to be freeze-dried and easily deployed at the point of need.^{17–19} These sensors take advantage of cellular machinery to detect small molecules and ions. Additionally, these reactions are relatively shelf-stable, disposable, and biodegrad-

Received: October 13, 2024

Revised: March 1, 2025

Accepted: March 3, 2025

Published: March 12, 2025



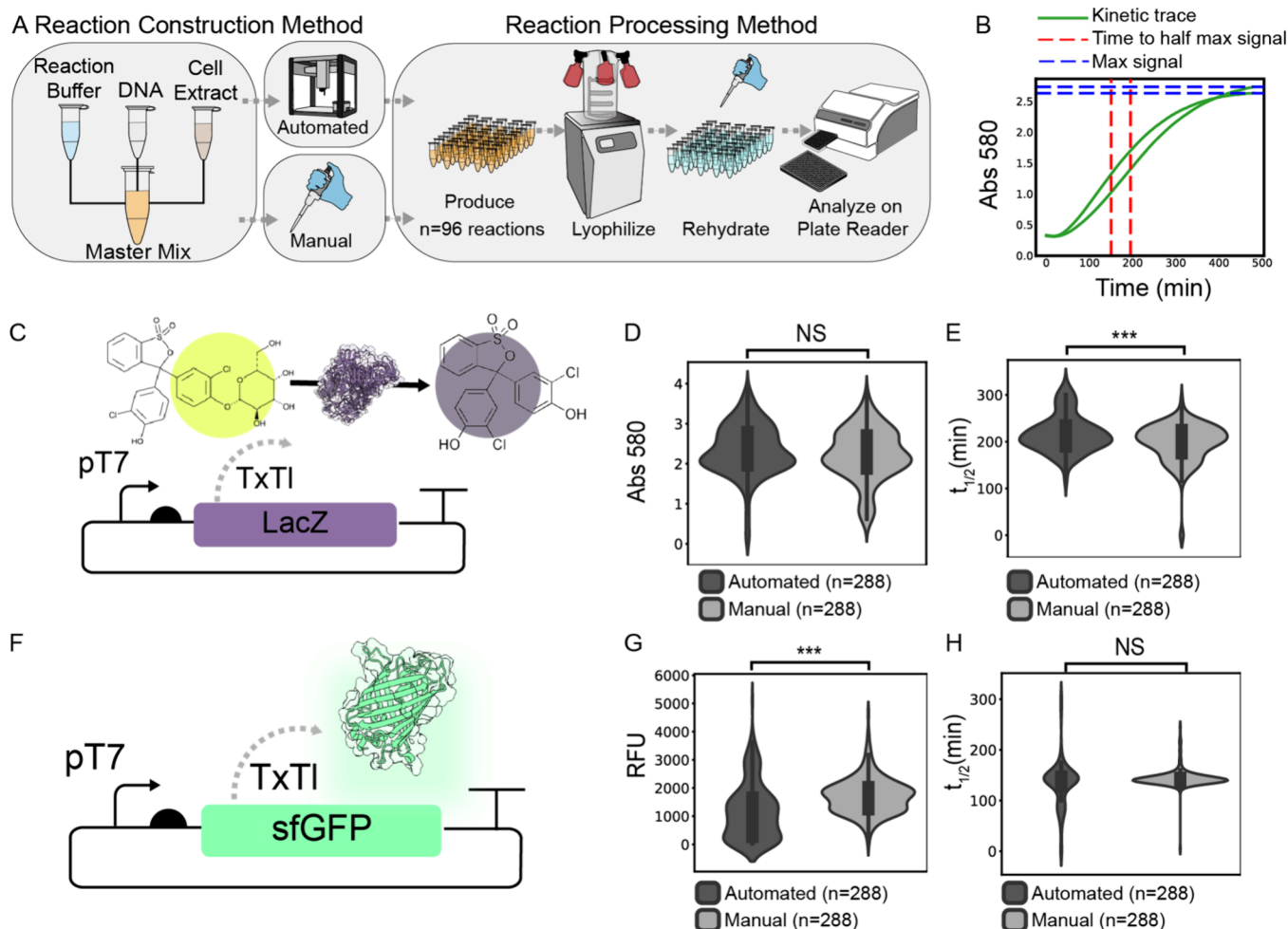


Figure 1. Characterization of manual and robotic construction of cell-free reactions. (A) Schematic of master mix reaction construction methods for manual and automated approaches. (B) Representative example of the data processing method, where $t_{1/2}$ and maximum signal are calculated and stored for each kinetic curve (two shown) in a cell-free reaction population. (C) Schematic of constitutive LacZ expression producing a colorimetric signal. (D, E) Violin plots showing (D) maximum colorimetric signal and (E) $t_{1/2}$ values from constitutive LacZ-producing reactions for $n = 288$ manual and $n = 288$ automated reactions. For each set of 288 reactions, three different experimenters constructed 96 of these reactions. (F) Schematic of constitutive T7 GFP expression producing a fluorescent signal. (G, H) Violin plots showing (G) maximum fluorescent signal and (H) $t_{1/2}$ values from constitutive GFP-producing reactions for $n = 288$ manual reactions and $n = 288$ automated reactions. For each set of 288 reactions, three different experimenters constructed 96 of these reactions.

able.^{20–25} Cell-free biosensors have demonstrated functionality in field deployment applications, being used to detect copper in water from California and fluoride levels in water from Kenya and Costa Rica as well as for educational purposes in high schools.^{26–29}

In each of these studies, cell-free biosensors were manufactured manually, and sensor quality was variable, with reactions providing false positives and negatives, not turning on as anticipated, or not showing reproducible behavior,^{26–29} motivating the need to develop approaches that can produce easy-to-use field-deployable sensors with consistent quality at scale. This is particularly important in cases where rapid generation of these diagnostics is needed. Automated approaches that incorporate robotic liquid handlers have the potential to allow for higher numbers of sensors to be manufactured with expected quality consistency across production batches.³⁰

Here we sought to adapt these automated approaches to manufacture cell-free biosensors. We specifically chose the Opentrons OT-2 device as a platform that is widely used across

biology to improve experimental workflows, with the added advantage of its affordability compared to other robotics systems. Additionally, Opentrons devices have a low barrier to entry with a lower expertise requirement and the potential to be easily deployed for site-specific manufacturing. To investigate the use of the Opentrons OT-2 system for biosensor manufacturing, we first characterized nonoptimized robotic production compared to manual biosensor construction. We then developed an automated protocol to produce hundreds of biosensor reactions for detecting fluoride, which were confirmed to be functional with follow-on characterization. We anticipate that this strategy can be widely applied to other biosensor systems and general cell-free system applications, such as cell-free protein synthesis or cell-free metabolic engineering, and can be further scaled to meet application needs.

RESULTS

Automation can be used to improve reproducibility and standardize processes within synthetic biology.^{30–33} Automa-

tion workflows can be designed under a variety of regimes, where the method of reaction construction can greatly affect the manufacturing outcome. The first step of determining automation best practices is the selection of manufacturing regimes and factors that are best suited for process outcomes.^{34–36} To determine this, we used two different methods of reaction preparation: (i) manual reaction construction and (ii) automated construction with an Opentrons OT-2 liquid-handling robot. In addition, we explored two modes of assembly: individual mix and master mix approaches. The individual mix approach describes the process of transferring each reaction component (DNA, cell extract, and reaction buffer components) separately to their respective tubes. The master mix configuration uses premixed components, where the DNA, cell extract, and reaction buffer are combined and then distributed into the reaction tubes. Individual mixtures may allow for more flexibility of the reaction environment and for component variation, while the master mix approach is quicker and easier to carry out in bulk for reactions that are compositionally consistent. For a small set of reactions created by a trained experimenter, master and individual mix approaches perform similarly; however, for “out of the box”, unoptimized automated approaches, the individual mix method leads to more failures, whereas the master mix approach is closer to human performance (Supplemental Figure 1).

This led us to adopt the master mix approach, as biosensor reactions for a given target can be produced with a bulk mixture to create reactions with homogeneous compositions. To characterize robot performance at a larger scale before optimization, we assessed the performance of over 288 manually constructed reactions (a total of 96 reactions carried out by three different experimenters) and 288 robotically constructed reactions using default settings (a total of 96 reactions carried out by three different experimenters) for two different reporter systems, totaling 1152 reactions (Figure 1). We employed different experimenters to assess whether robotic construction could address variability in reaction performance imparted by manual construction by multiple individuals. Reaction master mixes were created manually and then either placed on the Opentrons robot for distribution or distributed by hand. Reactions were then lyophilized for 16 h and characterized the next day after rehydration (Figure 1A). Reactions were rehydrated manually, as opposed to using the Opentrons, to demonstrate how they would be used in field settings. To compare manual versus default robotic settings, we used two metrics indicative of reaction performance: the maximum signal and the time to reach half of the maximum signal ($t_{1/2}$) (Figure 1B).

To test the effects of different reporter systems, we constructed cell-free reactions that constitutively expressed either a LacZ enzymatic reporter that produces a colorimetric signal or a superfolder green fluorescent protein (sfGFP) reporter that produces a fluorescent signal (Figure 1C,F). For the enzymatic reporter, nonoptimized automated protocols showed significant differences in $t_{1/2}$ when compared across manual and automated construction approaches with non-significant differences in the maximum signal (Figure 1D,E). Alternatively, for the fluorescent protein reporter, we observed that $t_{1/2}$ characterization showed no significant differences between automated and manual approaches, but the variance in the maximum signal was significantly different between these conditions (Figure 1G,H). Overall, this shows that

kinetic properties were retained well for a fluorescent reporter, where variations mostly occur for the maximum signal response metric. For enzymatic reporters, the opposite was true, perhaps because the dye concentration thresholds the maximal signal that can be generated by these reactions. Additionally, $t_{1/2}$ and maximum signal have a poor linear correlation with each other (Supplemental Figure 2). Overall, these results demonstrate differences in robotic and human performance for different reporter systems. Additionally, robotic systems do not inherently improve the reaction consistency issues imparted by multiple experimenters when using unoptimized robot settings. This is further demonstrated when assessing reaction performance separately based on experimenter (Supplemental Figure 3). These findings were in part due to the number of reactions that were not dispensed or dispensed at wrong volumes in the automated setup. This also demonstrates the importance of characterizing automation and system failure modes in determining optimization strategies.

Because of the inconsistency in reaction performance using default robot settings, we developed a protocol to improve both reaction quality and reduce the burden of manual scale-up (Figure 2A). Because the reactions are viscous, we found that a variety of robot settings have effects on the master mix distribution into tubes, including the dispense and aspirate rates, number of mixes, volume of mixing, liquid blowout height, touch tip height, and dispense heights. Blowout, an Opentrons command, refers to the process of pushing air from the pipet after dispensing to remove excess liquid, while another Opentrons command called touch tip touches the sides of the reaction vessel walls to remove excess liquid that may remain on the tip after blowout. We observed that without modifying these robotic parameters, the reaction easily bubbled and got stuck in the pipet tips, causing aspiration errors for subsequent reactions. We saw that the use of blowout and touch tip commands allows the excess liquid to be removed and imparted into the reaction tubes. This also reduced issues with aspirating the correct liquid volume due to reaction accumulation. To further help remediate this issue, we included more tip changes to prevent accumulation of the reaction in the tips. We found that the combination of lower dispensing heights and dispense rate, blowing out excess cell-free expression (CFE) mix, and using the touch tip function allowed for better distribution.

To test this protocol, we constructed 384 fluoride riboswitch reactions and characterized subpopulations of these reactions with sodium fluoride (NaF) concentrations of 0, 0.25, and 1 mM (Figure 2B). The protocol can construct this number of reactions in approximately 30 min, with the user swapping out 96-well PCR plates. This substantially reduces the experimenter burden compared to manually constructing the reactions. The fluoride riboswitch populations were then assessed based on maximum signal after lyophilization. All reactions were successfully dispensed in this process, compared to previous experiments where automation sometimes missed dispensing reactions and was a common mode of reaction failure (Figure 1 and Supplemental Figures 1–3). From these results, we observed that sensor populations followed a more consistent distribution pattern compared to the preoptimized distributions (Figure 2C). Additional analysis showed that 65% of the 384 reactions turned on when exposed to 0.25 or 1 mM NaF, compared to 67% of the 384 reactions expected to turn on in the presence of NaF (Figure 2D). Previous work has shown that a fluorescence level of 0.5 μ M fluorescein

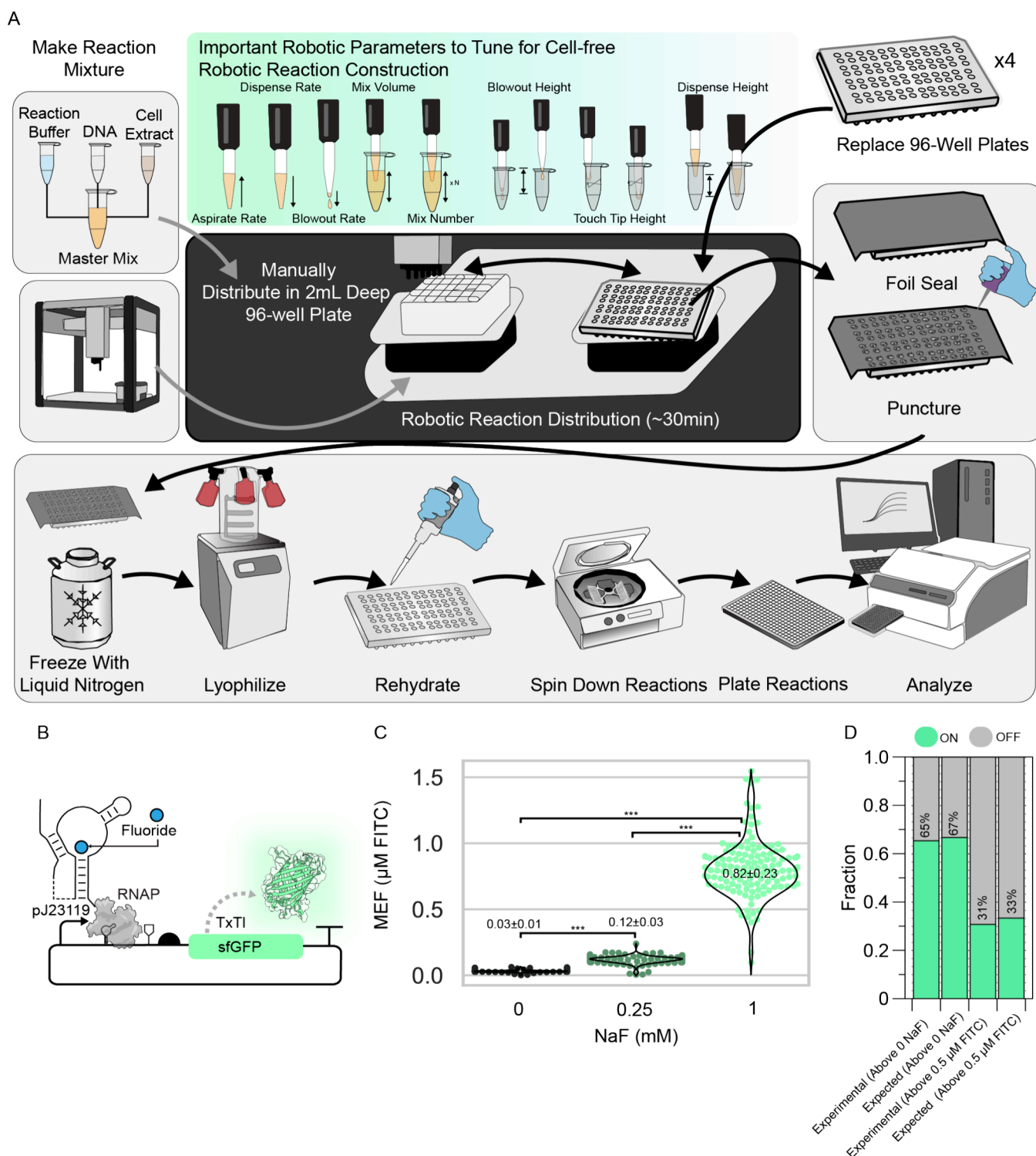


Figure 2. Characterization of robotic performance for constructing cell-free fluoride riboswitch biosensors. (A) Schematic of the semiautomated workflow for constructing hundreds of biosensor reactions using the Opentrons robotic device. (B) Schematic of the fluoride riboswitch biosensor mechanism. (C) Violin plot of maximum signal for $n = 384$ biosensor reactions. Three concentrations of fluoride were used to rehydrate the reactions distributed among 96-well plates using an interleaved-signal format to account for distribution effects. Average signal and standard deviation are shown in the plot for each condition. (D) Classification of reaction performance compared to expected performance using two different performance criteria. The first criterion represents the fraction of reactions that are expected to have a signal value higher than the maximum signal of the zero NaF condition, which are the 0.25 nM and 1 mM NaF conditions. The second criterion is used for biosensor field deployment metrics, where fluorescence can be visualized with a hand-held device when the signal is above 0.5 μM FITC. Here it is expected that only 1 mM NaF should meet this criterion.

isothiocyanate (FITC) calibrated signal is visible by eye with a detection device.²⁷ Therefore, we investigated the number of

reactions that met this condition (Figure 2D). Here we expected that the third of the 384 reactions exposed to 1 mM

NaF (33%) would reach the visualizable threshold and achieve a visualizable signal in 31% of the 384 reactions. Overall, we observed a reaction performance that was in line with the expected performance in reactions distributed by the OpenTrons OT-2 device.

DISCUSSION

There is a need to easily and accessibly scale up the production of cell-free systems such as cell-free biosensors for point-of-use applications. Here we present an approach that addresses this need by integrating easy-to-use robotics protocols to automate the assembly of reactions that can be freeze-dried in bulk before use by simple rehydration. We demonstrate this scale-up using the fluoride riboswitch, which has been previously deployed for point-of-use studies in Kenya and Costa Rica,^{28,29} showing that our approach can assemble hundreds of reactions that perform as expected.

We also found that automation does not necessarily improve process variability without optimization of the specific system. So, while automation may aid in scaling up, it is beneficial to optimize around quality control metrics and understand the limitations and failure modes of each system. We believe that the work carried out in this study demonstrates the process with which to determine and characterize constraints of cell-free systems upon integration with automation.

The tools described in this study can be adapted to a variety of cell-free reaction regimes, with the protocol designed to distribute reactions for 12 96-well plates at a time before needing to be restarted. This allows for producing upward of thousands of reactions, likely needing few modifications to the approach depending on the OpenTrons device and experimenter needs. As applications of cell-free manufacturing and biosensing become more realized, the ability to produce this scale of reactions in benchtop settings or lower-resourced environments becomes enabling.^{37–40} A particular selling point of the OpenTrons device is that it can be easily relocated and started up, which furthers applications for accessible point-of-use diagnostics production. This automated approach has the potential to reduce user error from manual methods that can have a large effect on batch-to-batch variation and can lead to consistent and expected experimental population behavior for the fluoride riboswitch.^{41,42}

To optimize the system, we needed to assess parameters that affect robotic performance when pipetting viscous liquids. As such, mixing rates, liquid blowout height, tip touch height, and swapping out multichannel pipet tips were all considered as factors that can be adjusted to reduce reaction failures and misfiring. It is important to consider these aspects when porting the protocol to other systems, and these parameters may be tuned depending on OpenTrons device differences, software versions, and reaction compositions. Additionally, it should be noted that rehydration procedures can also influence reaction outcomes, as they involve pipetting steps that can be subject to variability.

To facilitate adoption of this approach, we provide detailed protocols and OpenTrons operation code that implements the procedures described here. Our goal of this protocol is for it to serve as an accessible starting point to produce cell-free reactions at scales that match many application needs.

MATERIALS AND METHODS

Plasmids. For pT7 sfGFP synthesis, pJL1 (Addgene no. 69496) was used. For pY71-LacZ gene expression, a new plasmid was constructed. Plasmid pJBL3752 (Addgene no. 128809) was used for fluoride detection. Sequences for plasmids can be found in [Supplemental Table 1](#).

***E. coli* Lysate Production.** Lysate preparation was carried out using *E. coli* BL21(DE3)* for extract used in the fluoride riboswitch experiments and a Rosetta 2(DE3) $\Delta lacZ\alpha$ *E. coli* strain for the analysis in [Figure 1](#). Preparation for *E. coli* BL21(DE3)* extract was carried out using methods previously published.⁴³ Briefly, BL21(DE3)* cells were plated on agar, and a single colony was cultured overnight and then inoculated into 1 L of 2 \times YT + P media, composed of 16 g of tryptone, 10 g of yeast extract, 5 g of NaCl, 7 g of potassium phosphate dibasic, and 3 g of potassium phosphate monobasic. Cells were then grown with shaking at 220 rpm at 37 °C and harvested at an OD600 of 3.0, after approximately 4 h. Once an OD600 of 3.0 was reached, the cells were processed in accordance with the previous protocol up through dialysis.⁴³ A 100 L culture of Rosetta 2(DE3) $\Delta lacZ\alpha$ cells was processed for lysate production similar to the BL21(DE3)* lysate production mentioned previously but with modifications to accommodate production at scale. Briefly, 750 mL starter cultures (1.5 L total) were grown for 16 h at 37 °C with 200 rpm shaking incubation. Prior to inoculating 100 L of 2 \times YT + P culture media supplemented with 5 mL of antifoam 204 (Sigma, A8311) in an IF 150 L (New Brunswick Scientific) fermenter, the media was allowed to aerate overnight with a rotor speed of 100 rpm and 20 standard liters per minute (slpm) airflow at 37 °C. After inoculation with enough overnight culture to yield a starting OD600 of 0.05, the fermenter settings were adjusted to 300 rpm and 50 slpm, and the dissolved oxygen (DO) was calibrated to 100%. At an OD600 of 0.6–1.0, the culture was induced with a final concentration of 1 mM isopropyl β -D-1-thiogalactopyranoside (IPTG) (GoldBio, I2481C). Once the DO reached 50%, the rotor speed was increased to 500 rpm. At an OD600 of 3.5, the culture was cooled to 4 °C and centrifuged in a prechilled Powerfuge pilot 1.1 L bowl system (CARR Biosystems) within approximately 8 h, and the pelleted bacteria was subsequently processed as described previously.⁴³

Constitutive Cell-Free Reaction Assay. Reaction master mix for pT7-sfGFP and pY71-LacZ constitutive expression was carried out using a Cytomim master mix optimized by Cai et al., which contains 8 mM magnesium glutamate, 260 mM potassium glutamate, 1.26 mM AMP, 0.86 mM GMP, 0.86 mM UMP, 0.86 mM CMP, 4 mM oxalic acid, 2 mM L-glutathione, 1.5 mM spermidine, 9.2 mM potassium phosphate dibasic, 5.8 mM potassium phosphate monobasic, 2 mM amino acids, and 1 mM tyrosine.⁴⁴ The 11 μ L reactions were assembled using 4.4 μ L of Cai master mix, 3.3 μ L of cell extract, and 3.3 μ L of water with DNA concentrated to 15 nM in the complete reaction. For LacZ reporter reactions, 12.5 mM chlorophenol red β -D-galactopyranoside (CPRG) was also added to the water component of the reaction to a final volume of 0.88 μ L (1 mM concentration). Cell-free reactions were set up for 96 and 11 μ L reactions, with 20% dead volume for a total of 1267 μ L volume scaled proportionally to the volumes of individual reaction components listed above.

Cell-free expression reactions were carried out manually or using the default OpenTrons OT-2 settings. For manual expression, a master mix containing the above components

was made and hand-mixed 20 times using a p1000 pipet set to half the total volume (633 μL). The master mix was then distributed into 11 μL aliquots using a p20 pipet into 96 PCR tubes on ice. For robotic distributions, the master mix was made by hand without mixing and then placed on an Opentrons 24 1.5 mL tube rack. The robot was then made to mix the reaction 20 times at default rates using the Opentrons p1000 pipet attachment. The robot then distributed 11 μL of this master mix into 96 PCR tubes on a cooling module set to 4 $^{\circ}\text{C}$ using a p20 pipet attachment.

This process was completed by three separate experimenters using the same manual and automated protocol (see [Data Analysis Code and Statistics](#)). Once reactions were completed, they were immediately frozen with liquid nitrogen and placed on a Labconco FreeZone 2.5 L -84°C benchtop freeze-dryer for 16 h. Immediately after lyophilization, reactions were rehydrated with 11 μL of water using a multichannel pipet, spun down, mixed 20 times by hand, and plated on a 384-well plate. CPRG reporter reactions were then read at absorbance 585 nm wavelength at 5 min intervals for 480 min. Fluorescent reporter reactions were monitored using excitation/emission 485 nm/520 nm at 5 min intervals for 480 min. All reactions were analyzed at 30 $^{\circ}\text{C}$.

Fluoride Riboswitch Cell-Free Reaction Assay. Cell-free reactions for the fluoride riboswitch were carried out using a modified phosphoenolpyruvate, amino acids, NAD^+ , and oxalic acid (PANox)⁴⁵ reaction system with salt solution containing 8 mM magnesium glutamate, 10 mM ammonium glutamate, and 130 mM potassium glutamate; transcription master mix with 1.2 mM ATP, 0.850 mM GTP, 0.850 mM UTP, 0.850 mM CTP, 72 μM folinic acid, and 0.171 mg/mL tRNA; amino acids solution with 2 mM amino acids; energy solution of 30 mM PEP; and cofactor solution with 0.33 mM NAD, 0.27 mM CoA, 4 mM oxalic acid, 1 mM putrescine, 1.5 mM spermidine, and 57 mM HEPES.⁴³ The 11 μL reactions were assembled using 3.3 μL of PANox master mix, 3.3 μL of cell extract, and 4.4 μL of fluoride riboswitch DNA diluted in water to a final reaction concentration of 15 nM. The reactions were constructed using the master mix approach, where a bulk solution of 6083 μL was generated, including a 20% dead volume adjustment for robotic procedures. This reaction was then manually distributed in the first row of 2 mL 96 deep-well blocks with 760 μL of reaction in each well. This 96-well block was then placed on the Opentrons OT-2 platform for use by the protocol (see [Data Analysis Code and Statistics](#)). The Opentrons OT-2 platform configuration is shown in [Supplemental Figure 4](#). The reactions were distributed in 11 μL aliquots into 96-well PCR plates and kept on ice after distribution until all plates were completed, for a total of four plates. These plates were then simultaneously immersed in liquid nitrogen on 96-well aluminum PCR tube blocks and immediately placed on a Labconco FreeZone 2.5 L -84°C benchtop freeze-dryer for 16 h using a four-shelf lyophilization chamber. Immediately after lyophilization, the reactions were manually rehydrated with a multichannel pipet the next day with the indicated concentrations of NaF using an interleaved-signal format to account for positional effects further described in [Supplemental Figure 5](#). The reactions were then monitored using excitation/emission 485 nm/520 nm at 5 min intervals for 10 h at 30 $^{\circ}\text{C}$. To normalize the sfGFP signal, we used a NIST traceable fluorescein standard (Invitrogen F36915) and referred to this calibration as mean equivalent fluorescence (MEF) μM FITC throughout.

Data Analysis Code and Statistics. JMP Pro 16 was used to carry out nonparametric statistical analysis for data gathered in [Figures 1](#) and [2](#). Additionally, Python code for data analysis can be found at https://github.com/LucksLab/Brown_Phillips_Semi-Automated_Biosensor_Manufacturing_2024/tree/main with instructional and layout information on how to structure and carry out the Opentrons protocols found in [Figure 2](#) ([Supplemental Figures 4](#) and [5](#)). Opentrons protocols are available and annotated in the [Supporting Information](#).

■ ASSOCIATED CONTENT

Data Availability Statement

All data presented are available alongside code for analysis and Opentrons operation at https://github.com/LucksLab/Brown_Phillips_Semi-Automated_Biosensor_Manufacturing_2024/tree/main. Python code for data analysis as well as Opentrons protocols can be found at https://github.com/LucksLab/Brown_Phillips_Semi-Automated_Biosensor_Manufacturing_2024/tree/main. This contains Excel and Python files containing the raw data from [Figures 1](#) and [2](#) as well as output files and image files generated from the code. All code for data analysis was written with the assistance of OpenAI ChatGPT 3.5 and manually edited.

Supporting Information

The Supporting Information is available free of charge at <https://pubs.acs.org/doi/10.1021/acssynbio.4c00703>.

Supplementary table for DNA sequences, additional experimental data and analysis, and schematics of experimental configurations and protocols ([PDF](#))

■ AUTHOR INFORMATION

Corresponding Authors

Aleksandr E. Miklos – *Applied Synthetic Biology and Olfaction Branch, U.S. Army DEVCOM Chemical Biological Center, Gunpowder, Maryland 21010, United States*;
Email: aleksandr.e.miklos.civ@army.mil

Julius B. Lucks – *Department of Chemical and Biological Engineering and Center for Synthetic Biology, Northwestern University, Evanston, Illinois 60208, United States*;
orcid.org/0000-0002-0619-6505; Email: jblucks@northwestern.edu

Authors

Dylan M. Brown – *Department of Chemical and Biological Engineering and Center for Synthetic Biology, Northwestern University, Evanston, Illinois 60208, United States*

Daniel A. Phillips – *Applied Synthetic Biology and Olfaction Branch, U.S. Army DEVCOM Chemical Biological Center, Gunpowder, Maryland 21010, United States*

David C. Garcia – *Applied Synthetic Biology and Olfaction Branch, U.S. Army DEVCOM Chemical Biological Center, Gunpowder, Maryland 21010, United States*; *Precise Systems, Lexington Park, Maryland 20653, United States*;
orcid.org/0000-0002-6029-7964

Anibal Arce – *Department of Chemical and Biological Engineering and Center for Synthetic Biology, Northwestern University, Evanston, Illinois 60208, United States*;
orcid.org/0000-0001-8134-6385

Tyler Lucci – *Department of Chemical and Biological Engineering and Center for Synthetic Biology, Northwestern University, Evanston, Illinois 60208, United States*;
orcid.org/0009-0005-7324-4799

John P. Davies, Jr. – Decontamination Sciences Branch, U.S. Army DEVCOM Chemical Biological Center, Gunpowder, Maryland 21010, United States

Jacob T. Mangini – University of Maryland, College Park, Maryland 20742, United States

Katherine A. Rhea – Applied Synthetic Biology and Olfaction Branch, U.S. Army DEVCOM Chemical Biological Center, Gunpowder, Maryland 21010, United States

Casey B. Bernhards – Applied Synthetic Biology and Olfaction Branch, U.S. Army DEVCOM Chemical Biological Center, Gunpowder, Maryland 21010, United States;

orcid.org/0009-0005-2137-4081

John R. Biondo – Applied Synthetic Biology and Olfaction Branch, U.S. Army DEVCOM Chemical Biological Center, Gunpowder, Maryland 21010, United States; Precise Systems, Lexington Park, Maryland 20653, United States

Steven M. Blum – Applied Synthetic Biology and Olfaction Branch, U.S. Army DEVCOM Chemical Biological Center, Gunpowder, Maryland 21010, United States

Stephanie D. Cole – Applied Synthetic Biology and Olfaction Branch, U.S. Army DEVCOM Chemical Biological Center, Gunpowder, Maryland 21010, United States

Jennifer A. Lee – Applied Synthetic Biology and Olfaction Branch, U.S. Army DEVCOM Chemical Biological Center, Gunpowder, Maryland 21010, United States; Defense Threat Reduction Agency, Fort Belvoir, Virginia 22060, United States

Marilyn S. Lee – Applied Synthetic Biology and Olfaction Branch, U.S. Army DEVCOM Chemical Biological Center, Gunpowder, Maryland 21010, United States; orcid.org/0000-0002-4555-4803

Nathan D. McDonald – Biomufacturing Branch, U.S. Army DEVCOM Chemical Biological Center, Gunpowder, Maryland 21010, United States; orcid.org/0000-0003-3650-9493

Brenda Wang – Department of Chemical and Biological Engineering and Center for Synthetic Biology, Northwestern University, Evanston, Illinois 60208, United States

Dale L. Perdue – Department of Chemical and Biological Engineering and Center for Synthetic Biology, Northwestern University, Evanston, Illinois 60208, United States

Xavier S. Bower – Department of Chemical and Biological Engineering and Center for Synthetic Biology, Northwestern University, Evanston, Illinois 60208, United States

Walter Thavarajah – Department of Chemical and Biological Engineering and Center for Synthetic Biology, Northwestern University, Evanston, Illinois 60208, United States;

orcid.org/0000-0002-6122-2796

Ashty S. Karim – Department of Chemical and Biological Engineering and Center for Synthetic Biology, Northwestern University, Evanston, Illinois 60208, United States;

orcid.org/0000-0002-5789-7715

Matthew W. Lux – Applied Synthetic Biology and Olfaction Branch, U.S. Army DEVCOM Chemical Biological Center, Gunpowder, Maryland 21010, United States

Michael C. Jewett – Department of Chemical and Biological Engineering and Center for Synthetic Biology, Northwestern University, Evanston, Illinois 60208, United States; Department of Bioengineering, Stanford University, Stanford, California 94305, United States; orcid.org/0000-0003-2948-6211

Complete contact information is available at:

<https://pubs.acs.org/10.1021/acssynbio.4c00703>

Author Contributions

[#]D.M.B. and D.A.P. contributed equally. D.M.B., J.B.L., D.A.P., D.C.G., and A.E.M. designed the study. D.M.B, T.J.L., A.A.M., and D.A.P. carried out experimental work reported here. D.M.B., J.T.M., D.A.P, and D.C.G. developed OpenTrons protocols used in the study. D.M.B developed analytical code. J.P.D., D.A.P., D.C.G, and J.T.M. determined important robotic system parameters for tuning. K.A.R. and J.R.B. generated materials and lysate scale-up procedures used within. M.S.L., W.T., C.B.B., S.M.B., S.D.C, J.A.L., N.D.M., B.W., and D.L.P. aided in experimentation and procedure development. J.B.L., A.E.M., M.C.J., A.S.K., and M.W.L. supervised the study and acquired funding. D.M.B., D.A.P., J.B.L., and A.E.M. wrote the manuscript. All of the authors edited the manuscript.

Notes

The authors declare the following competing financial interest(s): W.T., J.B.L. and M.C.J. have submitted an international patent application that has been nationalized in the USA (US 17/309,240, US 17/593,026) relating to fluoride riboswitch biosensing, and J.B.L. and M.J.C. have submitted an international patent application that has been nationalized in the USA (US 62/714,427, US 17/265,785) related to cell-free biosensors. M.C.J. and J.B.L. are co-founders and have financial interest in Stemloop, Inc. The latter interests are reviewed and managed by Northwestern University in accordance with their conflict-of-interest policies.

ACKNOWLEDGMENTS

This work was supported by Army Contracting Command (W52PIJ-21-9-3023 to J.B.L.), the National Science Foundation (23110382 to J.B.L. and 2021900 to T.J.L.), and the Army Research Office (W911NF-22-2-0246 to M.C.J.). J.B.L. was also supported by a John Simon Guggenheim Fellowship. The views, opinions, and/or findings expressed are those of the authors and should not be interpreted as representing the official views or policies of the Department of Defense, the National Science Foundation, or the U.S. Government.

REFERENCES

- (1) Carvalho, F. P. Pesticides, environment, and food safety. *Food Energy Secur.* **2017**, *6*, 48–60.
- (2) Carvalho, F. P. Agriculture, pesticides, food security and food safety. *Environ. Sci. Policy* **2006**, *9*, 685–692.
- (3) Md Meftaul, I.; Venkateswarlu, K.; Dharmarajan, R.; Annamalai, P.; Megharaj, M. Pesticides in the urban environment: A potential threat that knocks at the door. *Sci. Total Environ.* **2020**, *711*, 134612.
- (4) Rizzo, D. M.; Lichtveld, M.; Mazet, J. A. K.; Togami, E.; Miller, S. A. Plant health and its effects on food safety and security in a One Health framework: four case studies. *One Health Outlook* **2021**, *3*, 6.
- (5) *Guidelines for Drinking-Water Quality*, 4th ed., incorporating the 1st addendum; World Health Organization, 2017.
- (6) *Human Exposure and Health*. U.S. Environmental Protection Agency. <https://www.epa.gov/report-environment/human-exposure-and-health>.
- (7) Eales, J.; et al. Human health impacts of exposure to phthalate plasticizers: An overview of reviews. *Environ. Int.* **2022**, *158*, 106903.
- (8) Sharma, N.; Singhvi, R. Effects of Chemical Fertilizers and Pesticides on Human Health and Environment: A Review. *Int. J. Agric. Environ. Biotechnol.* **2017**, *10*, 675.
- (9) Fuller, R.; et al. Pollution and health: a progress update. *Lancet Planet. Health* **2022**, *6*, e535–e547.

- (10) Rovira, J.; Domingo, J. L. Human health risks due to exposure to inorganic and organic chemicals from textiles: A review. *Environ. Res.* **2019**, *168*, 62–69.
- (11) Chartres, N.; Bero, L. A.; Norris, S. L. A review of methods used for hazard identification and risk assessment of environmental hazards. *Environ. Int.* **2019**, *123*, 231–239.
- (12) *Collection of Methods*. U.S. Environmental Protection Agency. <https://www.epa.gov/measurements-modeling/collection-methods#3>.
- (13) Kaserzon, S. L.; Heffernan, A. L.; Thompson, K.; Mueller, J. F.; Gomez Ramos, M. J. Rapid screening and identification of chemical hazards in surface and drinking water using high resolution mass spectrometry and a case-control filter. *Chemosphere* **2017**, *182*, 656–664.
- (14) Schierenbeck, T. M.; Smith, M. C. Path to Impact for Autonomous Field Deployable Chemical Sensors: A Case Study of in Situ Nitrite Sensors. *Environ. Sci. Technol.* **2017**, *51*, 4755–4771.
- (15) Benasco, A. R.; et al. Receptor Induced Doping of Conjugated Polymer Transistors: A Strategy for Selective and Ultrasensitive Phosphate Detection in Complex Aqueous Environments. *Adv. Electron. Mater.* **2022**, *8*, 2101353.
- (16) Clark, R. B.; Dick, J. E. Towards deployable electrochemical sensors for per- and polyfluoroalkyl substances (PFAS). *Chem. Commun.* **2021**, *57*, 8121–8130.
- (17) Thavarajah, W.; et al. A primer on emerging field-deployable synthetic biology tools for global water quality monitoring. *npj Clean Water* **2020**, *3*, 18.
- (18) Carlson, E. D.; Gan, R.; Hodgman, C. E.; Jewett, M. C. Cell-free protein synthesis: Applications come of age. *Biotechnol. Adv.* **2012**, *30*, 1185–1194.
- (19) Silverman, A. D.; Karim, A. S.; Jewett, M. C. Cell-free gene expression: an expanded repertoire of applications. *Nat. Rev. Genet.* **2020**, *21*, 151–170.
- (20) Arce, A. Decentralizing Cell-Free RNA Sensing with the Use of Low-Cost Cell Extracts. *Front. Bioeng. Biotechnol.* **2021**, *9*, No. 727584.
- (21) Warfel, K. F.; et al. A Low-Cost, Thermostable, Cell-Free Protein Synthesis Platform for On-Demand Production of Conjugate Vaccines. *ACS Synth. Biol.* **2023**, *12*, 95–107.
- (22) Stark, J. C.; et al. On-demand biomanufacturing of protective conjugate vaccines. *Sci. Adv.* **2021**, *7*, No. eabe9444.
- (23) Pardee, K.; et al. Paper-Based Synthetic Gene Networks. *Cell* **2014**, *159*, 940–954.
- (24) Pardee, K.; et al. Portable, On-Demand Biomolecular Manufacturing. *Cell* **2016**, *167*, 248–259.
- (25) Pardee, K.; et al. Rapid, Low-Cost Detection of Zika Virus Using Programmable Biomolecular Components. *Cell* **2016**, *165*, 1255–1266.
- (26) Jung, K. J.; et al. At-home, cell-free synthetic biology education modules for transcriptional regulation and environmental water quality monitoring. *ACS Synth. Biol.* **2023**, *12*, 2909–2921.
- (27) Jung, J. K.; et al. Cell-free biosensors for rapid detection of water contaminants. *Nat. Biotechnol.* **2020**, *38* (38), 1451–1459.
- (28) Thavarajah, W.; et al. Point-of-Use Detection of Environmental Fluoride via a Cell-Free Riboswitch-Based Biosensor. *ACS Synth. Biol.* **2020**, *9*, 10–18.
- (29) Thavarajah, W.; et al. The accuracy and usability of point-of-use fluoride biosensors in rural Kenya. *npj Clean Water* **2023**, *6*, 5.
- (30) Jessop-Fabre, M. M.; Sonnenschein, N. Improving reproducibility in synthetic biology. *Front. Bioeng. Biotechnol.* **2019**, *7*, 18.
- (31) Beal, J.; et al. Reproducibility of Fluorescent Expression from Engineered Biological Constructs in *E. coli*. *PLoS One* **2016**, *11*, No. e0150182.
- (32) Bultelle, M.; Casas, A.; Kitney, R. Engineering biology and automation—Replicability as a design principle. *Eng. Biol.* **2024**, *8* (4), 53–68.
- (33) Lux, M. W.; Strychalski, E. A.; Vora, G. J. Advancing reproducibility can ease the ‘hard truths’ of synthetic biology. *Synth. Biol.* **2023**, *8*, No. ysad014.
- (34) Hofmann, P.; Samp, C.; Urbach, N. Robotic process automation. *Electron. Mark.* **2020**, *30*, 99–106.
- (35) Syed, R.; et al. Robotic Process Automation: Contemporary themes and challenges. *Comput. Ind.* **2020**, *115*, 103162.
- (36) Herm, L. V.; et al. A framework for implementing robotic process automation projects. *Inf. Syst. E: Bus. Manage.* **2023**, *21*, 1–35.
- (37) Thames, A. H.; et al. A Cell-Free Protein Synthesis Platform to Produce a Clinically Relevant Allergen Panel. *ACS Synth. Biol.* **2023**, *12*, 2252–2261.
- (38) DeWinter, M. A.; et al. Point-of-Care Peptide Hormone Production Enabled by Cell-Free Protein Synthesis. *ACS Synth. Biol.* **2023**, *12*, 1216–1226.
- (39) Ji, X.; Liu, W.-Q.; Li, J. Recent advances in applying cell-free systems for high-value and complex natural product biosynthesis. *Curr. Opin. Microbiol.* **2022**, *67*, 102142.
- (40) Hu, V. T.; Kamat, N. P. Cell-free protein synthesis systems for vaccine design and production. *Curr. Opin. Biotechnol.* **2023**, *79*, 102888.
- (41) Cole, S. D.; et al. Quantification of Interlaboratory Cell-Free Protein Synthesis Variability. *ACS Synth. Biol.* **2019**, *8*, 2080–2091.
- (42) Rhea, K. A.; et al. Variability in cell-free expression reactions can impact qualitative genetic circuit characterization. *Synth. Biol.* **2022**, *7*, No. ysac011.
- (43) Silverman, A. D.; Kelley-Loughnane, N.; Lucks, J. B.; Jewett, M. C. Deconstructing Cell-Free Extract Preparation for in Vitro Activation of Transcriptional Genetic Circuitry. *ACS Synth. Biol.* **2019**, *8*, 403–414.
- (44) Cai, Q.; et al. A simplified and robust protocol for immunoglobulin expression in *Escherichia coli* cell-free protein synthesis systems. *Biotechnol. Prog.* **2015**, *31*, 823–831.
- (45) Kim, D.-M.; Swartz, J. R. Regeneration of adenosine triphosphate from glycolytic intermediates for cell-free protein synthesis. *Biotechnol. Bioeng.* **2001**, *74*, 309–316.